Effects of right pre-SMA rTMS on the Speed-Accuracy Tradeoff in Two Alternative Forced Choice Perceptual Decision Making

by

Tuğçe Tosun

A Thesis
Submitted to the Graduate School of Social Sciences and Humanities
through the Department of Psychology
in Partial Fulfillment of the Requirements for
the Degree of Master of Arts
at Koç University

March, 2016

Koç University

Graduate School of Social Sciences and Humanities

This is to certify that I have examined this copy of a master's thesis by

Tuğçe Tosun

and have found that it is complete and satisfactory in all respects,

and that any and all revisions required by the final

examining committee have been made.

Committee Members:

Assoc. Prof. Fuat Balcı

Asst. Prof. Tilbe Göksun

Asst. Prof. Patrick Simen

Date: 31/03/2016

STATEMENT OF AUTHORSHIP

This thesis contains no material which has been accepted for any award or any other degree or diploma in any university or other institution. It is affirmed by the candidate that, to the best of her knowledge, the thesis contains no material previously published or written by another person, except where due reference is made in the text of the thesis.

The author acknowledges that copyright of published works contained within this thesis resides with the copyright holder(s) of those works.

Signature

Tuğçe Tosun

ABSTRACT

The decision processes in two-alternative scenarios can be explained by the drift-diffusion model. According to this model, a decision variable moves towards one of two decision boundaries corresponding to the two alternatives based on the evidence accumulated in favor of these options and a decision is made when one of the decision boundaries is hit. However, the noise in the evidence accumulation process creates randomness in the trajectory of the decision variable which might result in hitting the wrong decision boundary. This leads to the speed-accuracy tradeoff (SAT) which is modulated by how high the decision boundaries are set. While higher threshold setting increases the likelihood of an accurate decision at the cost of longer response times, lower threshold setting results in less accurate but faster decisions. Recent neuroimaging studies showed that the activity of pre-supplementary motor area (pre-SMA) and striatum was higher when speed was emphasized compared to when accuracy was emphasized. Additionally, the activity in these brain regions was negatively linked with decision thresholds. However, the imaging studies provide only correlational information. In the current study, we aimed to draw a causal relationship between the pre-SMA activity and threshold setting by inhibiting the activity in this region using rTMS. Participants performed random dot motion task after pre-SMA or vertex (control condition) inhibition and decision thresholds for both rTMS sessions were estimated by the drift diffusion model. Our results revealed that under the pre-SMA inhibition condition, participants set higher decision thresholds and exhibited more cautious decisions compared to the control condition. Furthermore, the weight assigned to accuracy relative to reward was higher under the pre-SMA inhibition condition. Additionally, while the decision thresholds in the post-error trials were higher compared to the post-correct trials, this change did not differ between the conditions.

Keywords: Perceptual decision making, speed-accuracy tradeoff, pre-SMA, rTMS, drift-diffusion model

ÖZET

İki alternatifli bir senaryoda verilen kararlar sürüklenme-yayılım modeliyle açıklanabilmektedir. Bu modele göre bir karar değişkeni iki hipotez için toplanan kanıt ışığında bu iki hipoteze karşılık gelen karar eşikleriyle sınırlandırılmış bir alanda ilerler. Karar değişkeni bir eşiğe ulaştığında, o eşik ile ilişkilendirilmiş karar verilir. Ancak kanıt toplama sürecindeki gürültü, karar değişkeninin bazı durumlarda yanlış karar eşiğine ulaşmasına sebep olabilmektedir. Bu durum, karar eşiklerinin değiştirilmesi ile dengelenen hız-doğruluk ödünleşimine neden olmaktadır. Karar eşiğinin yükseltilmesi kararın doğruluk olasılığını artırıp süresini uzatırken, karar eşiğinin düşürülmesi doğruluk oranını düşürecek ancak karar hızını artıracaktır. Yakın zamanda yapılan beyin görüntüleme çalışmalarından elde edilen bulgular, pre-suplementer motor alan (pre-SMA) ve striatum aktivitesinin karar hızının vurgulandığı durumda karar doğruluğunun vurgulandığı duruma kıyasla daha yüksek olduğunu ve bu bölgelerdeki aktivite artışının karar eşiğindeki düşüşle ilintili olduğunu göstermiştir. Ancak görüntüleme çalışmaları nedensel bir ilişki kurmaya olanak vermediğinden çalışmamızda pre-SMA aktivitesini Tekrarlanan Transkraniyel Manyetik Stimülasyon (rTMS) yöntemiyle baskılayarak, bu bölgenin karar eşiğinin belirlenmesi üzerindeki nedensel rolünün incelemeyi amaçladık. Katılımcılar, pre-SMA veya verteks (kontrol durumu) alanları rTMS ile baskılandıktan sonra rasgele nokta hareketi prosedüründe test edilmiş ve her iki durum için de sürüklenme-yayılım modeli ile karar eşikleri tahmin edilmiştir. Sonuçlarımız, pre-SMA aktivitesi baskılandığında kontrol durumuna kıyasla daha yüksek karar eşikleri belirlendiğini ve daha ihtiyatlı karar verildiği göstermiştir. Ayrıca katılımcıların karar hızına karşılık doğruluğa atadıkları değerin pre-SMA aktivitesinin baskılandığı durumda kontrol durumuna göre daha yüksek olduğu gözlenmiştir, Bu bulgulara ek olarak, hata sonrası denemelerde karar eşikleri yükselirken, karar eşiklerinde görülen bu değişimin pre-SMA ve verteks uyarım durumlarına göre farklılaşmadığı görülmüştür.

Anahtar Sözcükler: Algısal karar verme, hız-doğruluk ödünleşimi, pre-SMA, rTMS, sürüklenme-yayılım modeli

ACKNOWLEDGEMENTS

First, I would like to express my special gratitude and thanks to my thesis advisor Dr. Fuat Balcı for his guidance and invaluable mentoring. I consider myself very lucky to have the opportunity to take part in his research team and to learn from his immense experience.

Secondly, I would like to thank Dr. Tilbe Göksun for her precious feedbacks on my research. I consulted her whenever I needed advice on my future research career and she never refrained to provide her warm and sincere support. I am also very grateful to Dr. Patrick Simen for his valuable suggestions and comments on my study.

I owe special thanks to Dr. Çağla Aydın and Dr. Mehmet Çakmak who encouraged me to apply for a master's degree in Psychology. It would be very difficult for me to make this important decision without their support and guidance.

I am also deeply grateful to my friend Dilara Berkay for her invaluable friendship and help in this study. Furthermore, I have learned a lot from all lab members and am very glad to work with them.

Last but not least, I would like to thank my family and Ahmet Emre Bayraktar for their endless love, patience and support.

TABLE OF CONTENTS

LIST OF TABLES

LIST OF FIGURES

1. INTRODUCTION

1.1. General Overview

Since many decisions are based on noisy evidence accumulation over time (Ratcliff, 1978; Shadlen & Newsome, 2001; Ratcliff & McKoon, 2008; Bogacz et al., 2010a), decision makers often face the dilemma between faster but more error-prone vs. more accurate but slower decisions (e.g., Bogacz et al., 2006). This phenomenon is referred to as the speed-accuracy tradeoff (SAT) (Fitts, 1966; Wickelgren, 1977). Importantly, maximizing reward rate in many decision scenarios entails optimizing this tradeoff. Although SAT has long been studied using mathematical models, such as the Drift Diffusion Model (DDM), the neural mechanisms of this adaptive function have not been extensively investigated (Bogacz et al., 2010a). Recent functional and structural imaging studies in which different response cautiousness levels were induced by emphasizing either speed or accuracy showed that cortico-basal ganglia circuitry, specifically the connections between pre-supplementary motor area (pre-SMA) and striatum, modulated SAT in perceptual decision making tasks (Ding & Gold, 2010; Forstmann et al., 2008; Forstmann et al., 2010; Green et al., 2012; Ivanoff et al., 2008; Lo & Wang, 2006; van Veen et al., 2008).

The current study aimed to investigate whether there is a causal relationship between the right pre-SMA activity and decision threshold setting and thus SAT. For this purpose, we manipulated the activity of the right pre-SMA using the continuous theta burst stimulation (cTBS) as the rTMS protocol prior to testing the participants in a two-alternative forced choice (2AFC) task. The response time and accuracy were modeled within the framework of the DDM to elucidate the effects of this manipulation on threshold setting. We hypothesized that the inhibition of right pre-SMA would lead to more cautious decisions by leading to wider decision boundaries.

1.2. Speed-Accuracy Tradeoff: Model-based Approaches

Neurophysiological and psychological data suggest that during perceptual decision making, the brain integrates sensory evidence supporting one alternative over the other over time before making a choice (Laming, 1968; Ratcliff, 1978; Roitman & Shadlen, 2002; Shadlen & Newsome, 2001). This integration process is required for accurate decisions because of the limited reliability of sensory evidence which stems from the noise in the sensory input and/or its transduction/processing. In a sense, this process can be treated as a statistical problem to be solved by the decision-maker (Stone, 1960).

Two-alternative forced choice perceptual decision making tasks such as the random dot motion discrimination (RDM) paradigm are widely used to investigate SAT. The RDM stimuli consist of moving dots a subgroup of which have a coherent motion towards either right or left (constituting signal) and the remaining of which move randomly (constituting noise). In this task, participants have to determine the direction of the coherent motion. Due to the noise in sensory evidence and its neural representation, participants have to accumulate information regarding the direction of the coherent motion in order to make an accurate decision. Keeping the task parameters constant within a block and using a fixed-length free response paradigm in which participants make their choices whenever they want, allow participants to develop block-based strategies regarding the speed and the accuracy of their choices (Bogacz et al., 2006).

The decision outputs gathered from this task can be modeled with different mathematical models. To this end, DDM is a widely used model of 2AFC although alternatives such as the Linear Ballistic Accumulator (LBA) exist (Brown & Heathcote, 2008). The DDM implements the optimum decision procedure for the 2AFC data (Laming, 1968) and assumes that the difference between the evidence from the noisy sources of sensory

information supporting the two alternatives is integrated over time, and when the accumulated information reaches one of the decision thresholds, either above or below the initial belief state (starting point), the corresponding option is chosen. SAT depends on the threshold parameter estimated by the DDM, which implies that due to the noise in the stimulus, higher thresholds lead to accurate but slower decisions (e.g., accuracy bias) whereas lower thresholds lead to faster but less accurate decisions (e.g., liberal bias).

1.3. Neural Basis of Speed-Accuracy Tradeoff

Studies regarding the role of cortico-basal ganglia circuitry, more specifically cortico-striatal connections, in the modulation of SAT constitute the majority of the investigations on the neural basis of this adaptive behavior (Bogacz & Gurney, 2007; Brown et al., 2004; Frank, 2006; Gurney et al., 2004; Lo & Wang, 2006; Standage et al., 2014). One of the constituents of this circuitry, basal ganglia are a group of subcortical nuclei involved in the control of voluntary actions (Redgrave et al., 1999). At the resting state, the globus pallidus interna, the output nuclei of the basal ganglia, inhibits the thalamus, and consequently the cortical areas, so that no premature responses are executed (Chevalier, Deniau & Desban, 1985; DeLong & Wichmann, 2007; Deniau & Chevalier, 1985). Striatum, the input nuclei of the basal ganglia, is activated when it receives consistent information supporting a particular action from cortical regions and this activation exerts a selective suppression on the globus pallidus. Through this suppression of the inhibitory effect of globus pallidus, associated cortical regions are released from inhibition, which leads to action execution (Chevalier, Deniau & Desban, 1985; Deniau & Chevalier, 1985). Hence, the basal ganglia are proposed to implement an action-selection mechanism that disinhibits the desirable actions while maintaining inhibitory control over others (Forstmann et al., 2008).

The main suggestion of the neuro-computational models of decision making (Bogacz & Gurney, 2007; Brown et al., 2004; Frank, 2006; Gurney et al., 2004; Lo & Wang, 2006) is that basal ganglia decreases its inhibitory control over the cortex when people have to make decisions under time pressure, which in turn facilitates fast but possibly premature decisions. Among the hypotheses proposed to explain the control of SAT in the cortico-basal ganglia circuitry, most prominent ones are the striatal and the subthalamic nucleus (STN) theories. The striatal theory proposes that when speed instructions are given, non-integrator cortical neurons (e.g., pre-SMA) send excitatory signals to the striatum. Increased striatal activity reduces the inhibitory effect of the basal ganglia over the thalamus and its target cortical areas, which in turn allows the execution of faster but often premature responses (Bogacz et al., 2010a; Forstmann et al., 2008). On the other hand, the STN theory posits that when accuracy of the responses is emphasized, frontal cortical areas (e.g., anterior cingulate cortex) send additional excitatory input to STN, which in turn increases the inhibitory control of basal ganglia over thalamus and cortex, leading to slower and thus more accurate decisions (Aron & Poldrack, 2006; Bogacz et al., 2010a; Frank, Scheres & Sherman, 2007). Taken together, striatal and STN pathways control SAT by decreasing or increasing the basal ganglia activity, respectively. Consequently, both approaches can account for threshold setting (not necessarily in a mutually exclusive fashion).

Several functional magnetic resonance imaging (fMRI) studies provided strong evidence regarding the dynamics of the relationship between cortical regions, particularly pre-SMA, and striatum to explain the modulation of SAT (Forstmann et al., 2008; Forstmann et al., 2010; Ivanoff et al., 2008; Mansfield et al., 2011; van Veen et al., 2008). For instance, Forstmann et al. (2008) observed a stronger BOLD signal in the right pre-SMA and striatum in response to a pre-trial instruction emphasizing the speed in an RDM task, compared to the conditions in which either accuracy was emphasized or no instruction was given.

Furthermore, they also found a significant correlation between the modulation of decision threshold parameter obtained from LBA fits of the data and activation in the right pre-SMA and striatum. In other words, greater hemodynamic response was observed in these brain regions of the participants who could readily adjust their decision boundaries considering the task demands. Similarly, in an MEG study by Wenzlaf and her colleagues (2011), a negative correlation between decision boundary and right SMA activity was observed in a perceptual decision making task.

Particularly, participants who had lower change in BOLD signal in pre-SMA and striatum had higher decision thresholds when making decisions under time pressure. Despite the differences in the tasks, designs, decision-theoretic approaches and research focus, the studies of Ivanoff et al. (2008) and van Veen et al. (2008) revealed similar results indicating that sustained activity in striatum and right pre-SMA increased when the participants were instructed to respond quickly. This finding is compatible with the results of the investigations that show the pre-SMA was involved in the internal planning of action strategies and in the anticipation of a motor response (Hikosaka & Isoda, 2010; Nachev et al., 2008). None of these studies reported a change in the activity of the sensory cortical areas or the primary motor cortex. Thus, in agreement with the decision-theoretic approaches, fMRI studies suggest that SAT modulation is controlled by the brain areas which are involved in decision making such as cortico-basal ganglia circuitry (Bogacz & Gurney, 2007; Lo & Wang, 2006; Standage et al., 2014; Watanabe et al., 2015) rather than in early sensory or primary motor areas (Bogacz et al., 2010a; Ding & Gold, 2010).

Another line of evidence regarding the neural underpinnings of SAT comes from the structural imaging studies. The study of Forstmann et al. (2010) investigated the relationship between the individual differences in behavior and in the structural features of particular brain regions focusing on the striatal and STN theories. The results of this study revealed that the

participants who demonstrated larger adjustments of the decision boundary (i.e., who quickly changed their decision thresholds considering the task demands in an RDM task) had stronger connectivity between pre-SMA and striatum. On the other hand, they did not observe stronger connections from any cortical region to STN that lead to more flexible adjustments in decision thresholds. Thus, these findings did not provide support for the STN theory of SAT.

Based on the investigations supporting the role of cortico-basal ganglia circuitry in SAT, we inhibited the activity of right pre-SMA using rTMS, in order to examine whether there was a significant change in the decision thresholds of the participants compared to the condition in which another brain region (vertex) irrelevant to decision making was inhibited. Findings of a recent rTMS-fMRI study (Watanabe et al., 2015) supported our assumption on the causal links between pre-SMA and striatum, i.e. inhibition of pre-SMA changes the activity in the basal ganglia which have a key role in controlling SAT and modulation of the decision thresholds. The results of the study of Watanabe et al. (2015) revealed that rTMS of pre-SMA had a significant effect on the connectivity between pre-SMA and striatum, and between striatum and globus pallidus during a response inhibition task. They also observed that the behavioral changes observed in terms of response inhibition were correlated with the magnitudes of change in the resting state functional connectivity between these areas. These results indicated that there is a causal relationship between pre-SMA and globus pallidus via striatum during response inhibition, while no causal effects exist in the activity and functional interaction involving STN (Watanabe et al., 2015). To our knowledge, there is no rTMS study that tested the causal relationship between particular brain areas and the control of the SAT. The current study intended to fill this crucial gap in the literature.

2. METHODS

2.1. Participants

Twenty-four healthy volunteers (13 female), aged 19-24 years (M = 20.88, SD = 1.68) participated in the study. These participants met the TMS safety criteria (Rossi et al., 2009; Wasserman, 1998). Participants were recruited through a publicly available announcement published on the Koç University website. A pre-experimental health form was used to screen for contraindications of TMS. Any participant who did not meet the eligibility criteria was excluded from the experiment. All participants were right-handed and had normal or corrected-to-normal vision. None of the participants tested were taking medication or had previous or actual neurological disorder or history of psychiatric illness, drug or alcohol abuse. The study was approved by the Ethical Committee of Koç University. Written and oral informed consent was obtained from all participants.

2.2. Design

We used a within-subjects design in the experiment. All participants were tested in three fixed-duration random dot motion discrimination sessions all of which were held in different days. The first session was a behavioral session, while the second and the third sessions were either pre-SMA or vertex inhibition (cTBS) sessions applied in a counterbalanced order. All participants received monetary reward based on their performance.

2.3. Stimuli and Apparatus

The visual stimulus consisted of a circular field of randomly moving white dots (3x3 pixels) which appeared in a 3 inch diameter kinematogram in the center of the computer screen with a black background (see Gold & Shadlen, 2001; Shadlen & Newsome, 2001). On each trial, a particular portion of the dots moved either towards left or right with a fixed

speed, while the rest of the dots were randomly repositioned over time. The motion direction was assigned randomly with equal probability. The stimulus was generated in MATLAB and presented on an 18-in MAC monitor via Psychophysics Toolbox extension (Brainard, 1997; Pelli, 1997). Participants were seated approximately 60 cm from the monitor and reported their responses via computer keyboard presses.

For the brain stimulation, a Magstim magnetic stimulator (figure-eight coil, 70-mm-diameter double circle, air cooled) was used. Intensity and locations for rTMS application were determined for each participant prior to behavioral testing. The international 10-20 system for EEG electrode placement was utilized for the localization of the target brain sites. The relative distances of 10% or 20% of the individual distances from the vertex to the relevant landmarks was considered by 10-20 EEG caps by requiring exact adaptation of the cap to these landmarks (Herwig et al., 2003). EEG caps with 74 positions designed according to the 10-20 system (The g.GAMMAcap, G.Tec Medical Engineering GMBH, Austria) were used to define the 10-20 positions. Considering the variation in the individual head sizes of the participants, the cap with appropriate size (either medium: 54-58 cm or large: 58-62 cm) was chosen.

2.4. Procedure

2.4.1. Free-Response Dot Motion Discrimination

In each session, the experiment comprised nine 4-min test blocks of free-response (FR) dot motion discrimination task with 8% motion coherence, and two 2-min signal detection (SD) blocks to determine non-decision times. Additionally, at the beginning of the first session, there was a 4-min practice block of dot motion discrimination task with 16% coherence. Participants were allowed to take a break of up to 4-min at the end of the test blocks.

For FR trials, participants were instructed to respond as quickly and accurately as possible by pressing the ‘M’ (for rightward) or ‘Z’ (for leftward) key on the computer keyboard to report their decisions regarding the direction of the coherent motion. In each trial, stimuli were terminated when a response was given. The response-to-stimulus interval (RSI) was sampled from a truncated exponential distribution with a mean of 2 s, a lower bound of 1 s, and an upper bound of 5.6 s. Correct responses were signaled by a short audio tone indicating positive feedback while incorrect responses were not followed by any feedback. Every correct response was awarded a point (corresponding to 4 kurus - approximately 2 cents), and there was no monetary penalty for errors. If the participants pressed the keys before the stimulus had been presented or their response time was lower than 100 ms (premature response), they were penalized by a 4-s timeout period, which started after a buzzing sound. After every 10 trials, the cumulative scores were displayed in the center of the screen.

For SD trials, participants were instructed to press the ‘M’ key in the first block and ‘Z’ key in the second block as soon as they saw the stimulus on the screen without considering the coherent motion. Each response was awarded 4 kurus unless it was premature.

2.4.2. rTMS Protocol

An off-line Theta Burst Stimulation (TBS) was applied over the target brain sites (either right pre-SMA or vertex in a counterbalanced order) at the beginning of the second and the third sessions. This protocol consists of 3 pulses of stimulation given at 50 Hz, repeated every 200 ms (Huang et al., 2005). The inhibition protocol was determined as continuous TBS (cTBS) which comprises a 40 s train of uninterrupted TBS (600 pulses) as described by Huang et al (2005). This protocol was prefered over the traditional rTMS protocol as it enables having a longer-lasting inhibitory effect with a considerably shorter stimulation duration (Huang et al.,2005; Hubl et al., 2008), which makes the stimulation more

comfortable for the participants. During stimulation, the coil was held in a fixed position by a mechanical arm over the stimulation sites. The brain region for vertex was determined as Cz site in the international 10-20 EEG system. For the localization of right pre-SMA, the center of the magnetic coil was placed over the Fz site (Cavazzana et al., 2015; Hsu et al., 2011). The exact point of stimulation was 1 cm lateral to the right from the mid-sagittal line. In previous studies, Talaraich coordinates of right pre-SMA was determined as (x, y, z) = (-4, 32, 51) (Chen et al., 2009; Conte et al., 2012; Li et al., 2006) which falls within the Fz site both in 10-10 system (Koessler et al., 2009) and in 10-20 system (Vitali et al., 2002). The number of participants allowed us to use the 10-20 system for localization (Sack et al., 2009).

In order to set the specific intensity of stimulation for each participant, single pulse TMS was applied at increasing intensities and the active motor threshold (AMT) of each individual was determined according to the criterion that a given intensity evokes a muscle twitch in the contralateral hand (Huang et al., 2005). For each participant, stimulation power was 80% of their AMT in both right pre-SMA and vertex inhibition conditions.

2.5. Data Analysis

The units of analysis were the accuracy and response time data obtained from the 2AFC task in the right pre-SMA and vertex inhibition sessions. Data from the behavioral session, in which no stimulation was applied, was not included in the analyses since this was a practice session aimed at establishing the steady-state performance. As these anticipatory responses do not reflect task representative behavior, we excluded the data from the trials with RTs below 100 ms (0.07% of all trials). Additionally, we specified a fixed probability for obtaining an outlier (assuming 5% of the RTs are outliers).

The final data were fit by the DDM using the within-subjects Hierarchical Bayesian estimation of DDM parameters (HDDM) in Python (Wiecki et al., 2013). HDDM is a more

accurate procedure to obtain DDM parameter estimates for both individuals and groups compared to the other methods, in which all individuals are assumed to be completely different or all same. In the Bayesian estimation procedure used in HDDM, quantification of parameter estimates is performed in the form of the posterior distributions which are approximated by Markov Chain Monte Carlo (MCMC) sampling methods (Frank et al., 2015). In order to obtain smooth parameter estimates, 10000 samples were drawn from the posterior distribution and the first 1000 were discarded as burn-in.

The data obtained from the right pre-SMA and vertex inhibition sessions were coded as within-subjects conditions. In order to test whether there was a difference in parameter estimates between the conditions, we determined the vertex inhibition condition as the baseline level and the model parameters for the pre-SMA inhibition condition were estimated in reference to this baseline. We fit three different models in all of which the decision threshold was allowed to vary between two experimental conditions.

The first model, in which only the decision threshold was allowed to vary was the most theoretically constrained model in terms of our hypothesis regarding the effect of pre-SMA rTMS on the decision process. For completeness, we also fit two other models in which drift rate or drift rate and non-decision time parameters were also allowed to vary between the conditions in addition to the threshold.

In order to evaluate the performance of our three alternative models with varying complexity, we used each model's Deviance Information Criterion (DIC). The DIC values for Model 1, 2 and 3 were 63484, 63478 and 63477, respectively. A model with lower DIC value performs better compared to the other models and a difference of 10 or greater between model DIC scores is interpreted as significant (Burnham & Anderson, 2003). Since the differences between the DIC values of the models were not higher than 10, none of the models performs significantly better than the other. Based on these model comparison

statistics and the specificity of our hypothesis, we present the results for Model 1 in the main text. The results for Model 2 and 3 are presented as Supplemental Information. It is important to note that the results of all model fits showed the robust effect of the pre-SMA rTMS on decision thresholds.

3. RESULTS

3.1. Response Time and Accuracy Comparisons

We first examined whether there was a difference in the response times and the accuracy levels between the right pre-SMA inhibition and the vertex inhibition conditions. Even though the change in both response times and accuracy levels were in the predicted directions (Table 2), these changes were not statistically significant ($t(23) = 1.20$, $p = .24$ and $t(23) = 1.15$, $p = .26$). In order to further investigate the strength of evidence in favor of the null findings obtained from the frequentist t-tests, we conducted Bayesian t-tests (Rouder et al., 2009). As the results revealed, the odds were 2.47:1 (weak evidence; Raftery, 1995) and 2.57:1 (weak evidence) in favor of the null hypothesis that there were no difference between conditions for the response times and the accuracy levels, respectively.

Table 1

Means and Standard Deviations of Response Times and Accuracy Levels in Right pre-SMA and Vertex Inhibition Conditions

	Response Times		Accuracy Levels	
Condition	*M*	*SD*	*M*	*SD*
Right pre-SMA Inhibition	1.00	0.25	0.78	0.13
Vertex Inhibition	0.96	0.27	0.76	0.11

3.2. Effects on the latent decision process

3.2.1. Model 1

To examine whether the latent decision processes associated with the control of the SAT has been affected by our experimental manipulation, we fit a drift diffusion model, in which only the decision threshold parameter was allowed to vary between the conditions.

We assessed the convergence of the MCMC chains from the starting point to the posterior distribution calculating the $\hat{R}$ (Gelman-Rubin) statistic from 5 separate runs (each containing 10000 samples) of the first model. All of the $\hat{R}$ values for all model parameters were lower than 1.1 indicating successful convergence. We also visually inspected the chains whether there was a convergence problem and confirmed that the chains had successfully converged.

Figure 1 shows the posterior distributions of the threshold parameter in the right pre-SMA inhibition condition with regard to the control condition Given the fact that Figure 1 shows the distribution of the difference between the pre-SMA and vertex rTMS conditions, the degree of overlap between the posterior distribution with the value of 0 can be used as the comparison metric. As the posterior distribution of this difference between conditions does not overlap with zero, we can conclude that the thresholds in the pre-SMA inhibition condition is significantly higher than the thresholds in the vertex inhibition condition ($p <$ .001). In other words, when the excitability of the right pre-SMA was reduced, participants set higher decision thresholds exhibiting a more cautious decision strategy. Additionally, we calculated the percentage difference between the means of the posterior distributions for the threshold parameter in pre-SMA and vertex inhibition conditions. The results of this analysis showed that the mean of the threshold parameter increased in the pre-SMA inhibition condition by 4.98% with respect to the control condition.

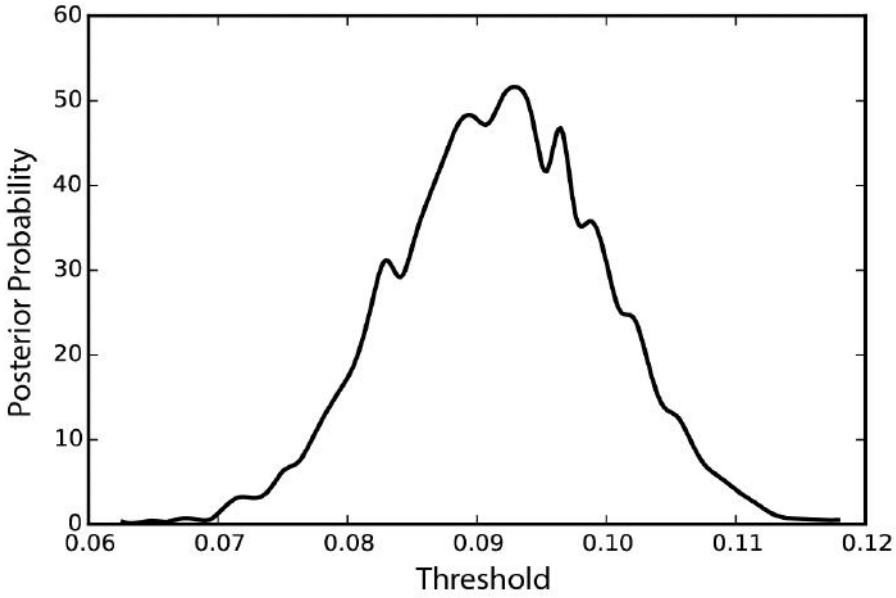

Figure 1. Posterior distribution of the threshold parameter estimated for pre-SMA inhibition condition with regard to the vertex inhibition condition. Peak values of the distribution represent the best estimates of the parameter, and the width of the distribution represents its uncertainty.

3.2.2. Model 2

In this model, decision threshold and drift rate parameters were allowed to differ between the conditions. The within-subjects effect of the pre-SMA inhibition condition on the decision threshold was examined as the posterior distribution of threshold parameter in pre-SMA condition with regard to the control condition which was determined as the baseline level. As seen in Figure 2, the posterior distribution of the threshold parameter does not overlap with zero indicating a significant effect of the condition on this parameter estimate (100% of posterior > 0). Since, the distribution was shifted to the right of 0 point, the decision threshold estimated for the pre-SMA condition is significantly higher than the threshold in the control condition. Thus, inhibition of right pre-SMA has a significant effect on the response cautiousness levels of the participants making them to set higher decision thresholds. This effect was is fully consistent with the findings gathered based on Model 1. Similarly, the within subjects effect of the pre-SMA inhibition on the drift rate parameter was also

significant (99% of posterior > 0; see Figure 3). This result indicated that participants had higher evidence accumulation rates when their right pre-SMA was inhibited compared to the condition in which their vertex was inhibited.

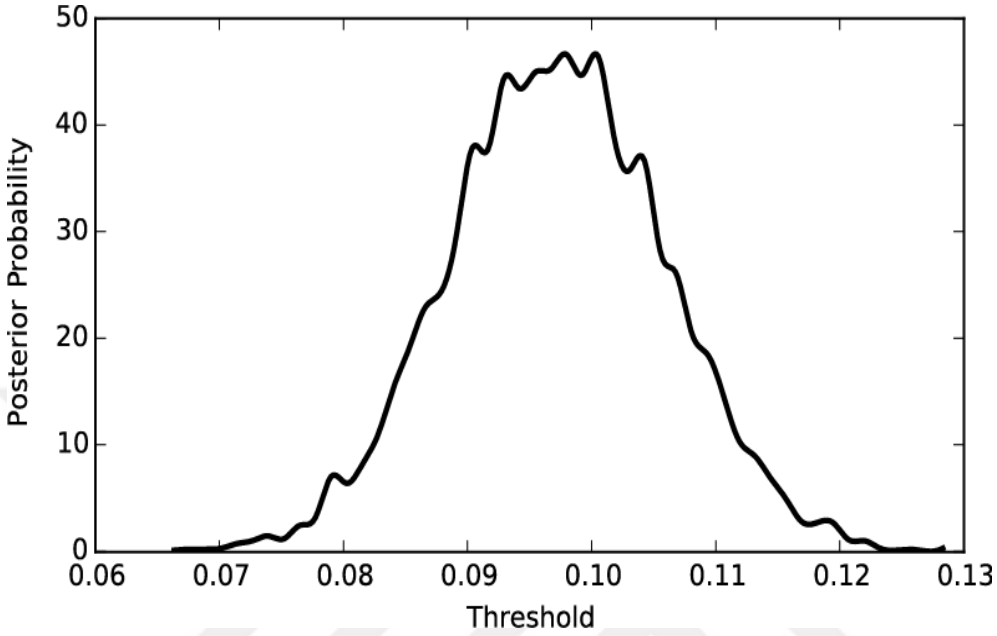

Figure 2. Posterior distribution of the threshold parameter estimated for pre-SMA inhibition condition with regard to the vertex inhibition condition for Model 2 where threshold and drift parameters were allowed to vary between conditions. Peak values of the distribution represent the best estimates of the parameter, and the width of the distribution represents its uncertainty.

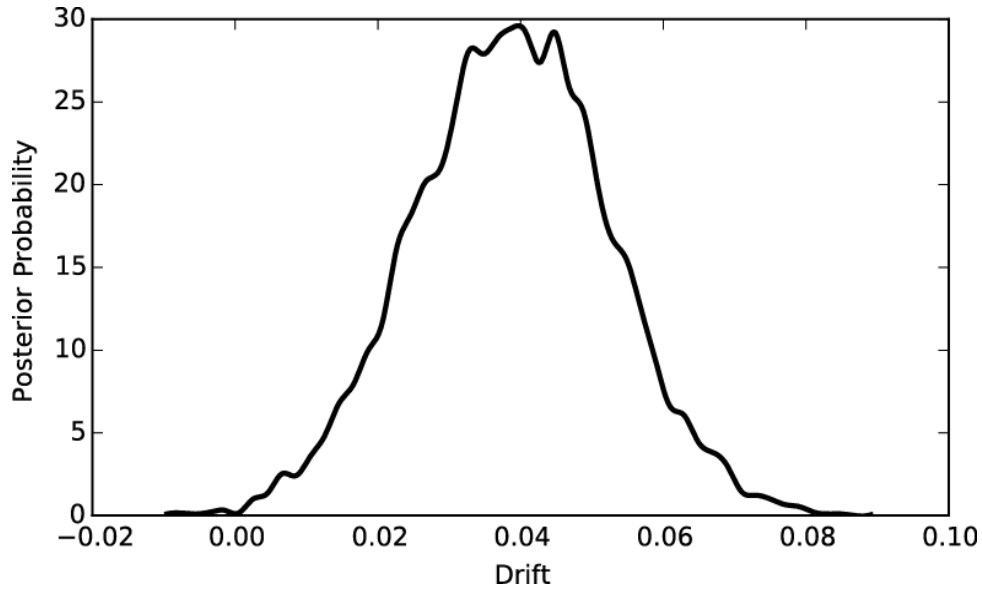

Figure 3. Posterior distribution of the drift parameter estimated for pre-SMA inhibition condition with regard to the vertex inhibition condition for Model 2 where threshold and drift parameters were allowed to vary between conditions.

We assessed the convergence of the MCMC chains calculating R-hat statistics and generating the graphs for each parameter and condition. Visual inspection of the figures of each chain and obtaining R-hat (Gelman-Rubin) values lower than 1.1 showed that all MCMC chains converged successfully.

Additionally, we calculated the percentage difference between the means of the posterior distributions for the threshold and drift rate parameters in pre-SMA and vertex inhibition conditions. The results of this analysis showed that the mean of the threshold parameter increased by 5.29% and the mean of the drift rate parameter increased by 5.13% in the pre-SMA inhibition condition with respect to the control condition.

3.2.3. Model 3

In this model, along with the threshold and drift rate parameters, non-decision time parameter was also allowed to vary across the conditions. Consistent with the results of the second model fits, threshold (100% of posterior > 0) and drift rate (99% of posterior > 0) was significantly higher in the pre-SMA inhibition condition compared to the vertex inhibition condition as seen in the Figure 4 and Figure 5 respectively. On the other hand, the within subjects effect of the right pre-SMA inhibition condition on the non-decision time parameter was not significant (94% of posterior < 0; see Figure 6). Therefore, we concluded that the non-decision time parameter was not affected by the decrease in the right pre-SMA activity.

For all parameters and conditions, the MCMC chains successfully converged from the starting point to the posterior distribution. All R-hat statistics were also lower than 1.1 indicating that there was no convergence problem in any parameter and condition.

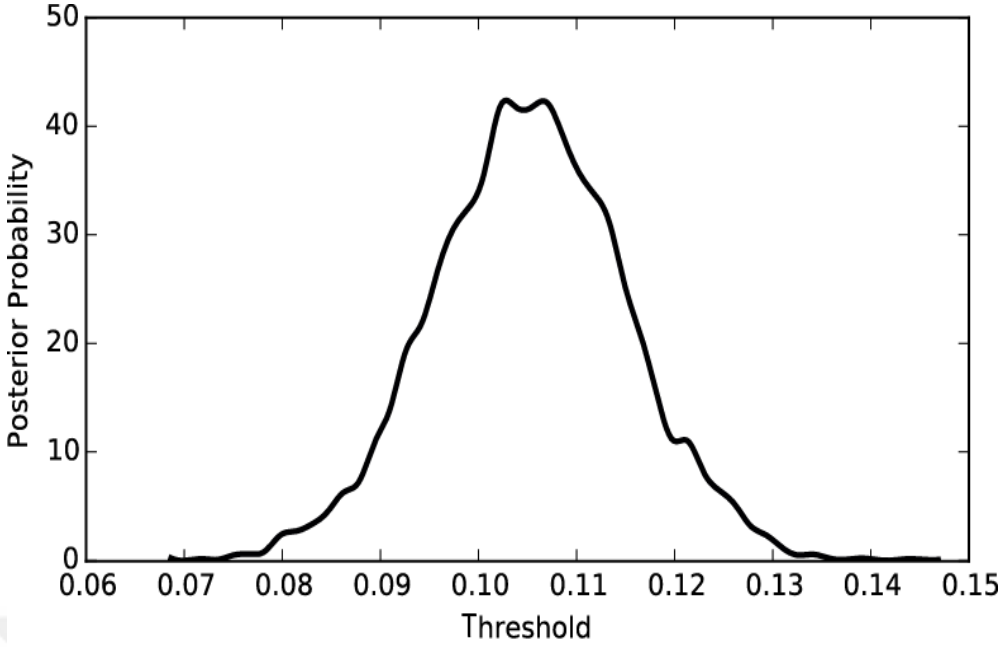

Figure 4. Posterior distribution of the threshold parameter estimated for pre-SMA inhibition condition with regard to the vertex inhibition condition for Model 3 where threshold, drift, and non-decision time parameters were allowed to vary between conditions.

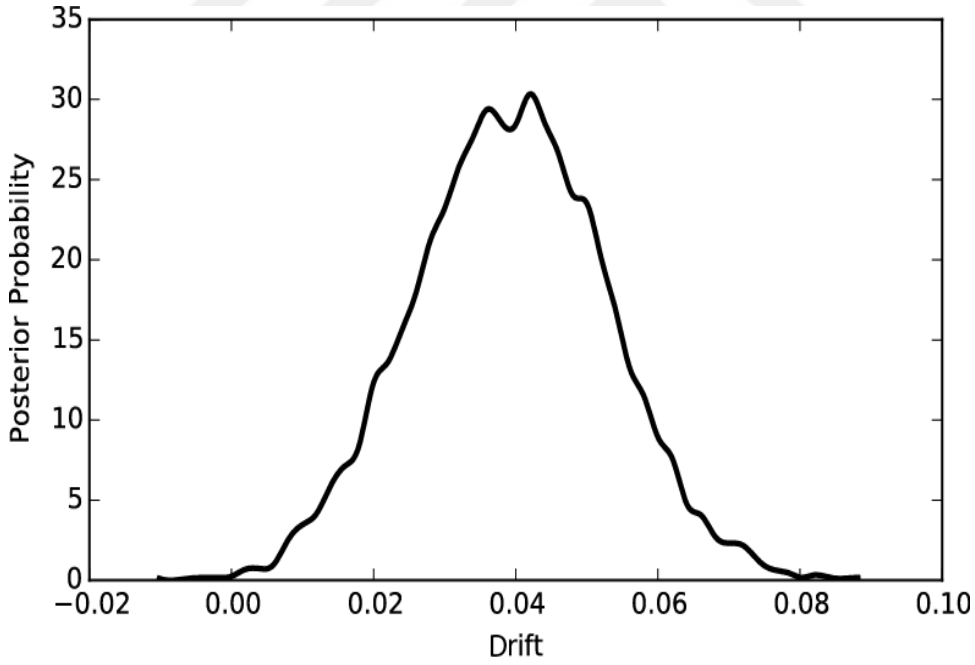

Figure 5. Posterior distribution of the drift parameter estimated for pre-SMA inhibition condition with regard to the vertex inhibition condition for Model 3 where threshold, drift, and non-decision time parameters were allowed to vary between conditions.

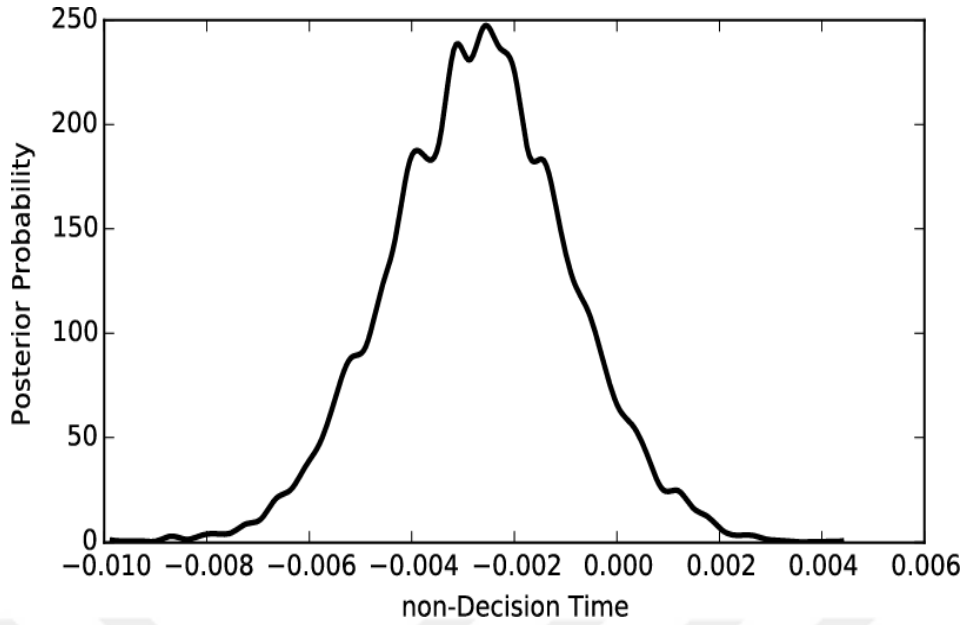

Figure 6. Posterior distribution of the non-decision time parameter estimated for pre-SMA inhibition condition with regard to the vertex inhibition condition for Model 3 where threshold, drift, and non-decision time parameters were allowed to vary between conditions.

Additionally, we calculated the percentage difference between the means of the posterior distributions for the threshold, drift rate and non-decision time parameters in pre-SMA and vertex inhibition conditions. The results of this analysis showed that the mean of the threshold parameter increased by 5.72%, the mean of the drift rate parameter increased by 5.15% while the mean of the non-decision time parameter decreased by 0.89% in the pre-SMA inhibition condition with respect to the control condition.

3.3. Speed-Accuracy Tradeoff & Reward Rate Maximization

Reward maximization in free-response fixed session time tasks require participants to find the optimal balance between the speed and the accuracy of their decisions. The expected reward rate (*RR*) in free-response 2AFC tasks is calculated as described below (Gold &Shadlen, 2002):

$$RR = \frac{1 - ER}{DT + T0 + RSI} \tag{1}$$

where *ER* denotes error rate, *DT* represents decision time, *T0* is time required for all non-decision related processes and *RSI* is the response-to-stimulus interval. *DT* is calculated by subtracting the non-decision related times from the response times. Reward maximizing mean-normalized decision times are calculated as below within the framework of reduced form of DDM (Bogacz et al., 2006):

$$\frac{DT}{Dtot} = \frac{1}{\frac{1}{ERlog\left(\frac{1-ER}{ER}\right)} + \frac{1}{1-2ER}} \tag{2}$$

where *Dtot = T0 + RSI*.

In 2AFC tasks, the majority of the participants were shown to set their decision thresholds higher than the reward maximizing thresholds predicted by the DDM early in training (Balcı et al., 2011; Bogacz et al., 2010b; Maddox & Bohil, 1998; Pitz & Reinhold, 1968; Stevenson et al., 1991). This accuracy bias was formulated by Bogacz et al. (2006) as below with an additional parameter in the reward rate function, which represents a penalty for error:

$$RR(q) = \frac{(1 - ER) - qER}{DT + Dtot} \tag{3}$$

where *q* represents the weight assigned to accuracy relative to the reward. Considering different error rates, the related normalized optimal decision times (given that *q* stands for an actual penalty) are calculated using the formula below (Bogacz et al., 2006):

$$\frac{DT}{Dtot} = (1+q)\frac{1}{\frac{1}{ER} - \frac{q}{(1-ER)}} + \frac{1-q}{1-2ER}$$

(4)

When q is equal to zero, Equation 4 prescribes the optimal performance curve for a task with no penalty for errors (as in the case of the current task) and thus the best fit q value indicates the degree of accuracy bias assuming that the participant optimizes this alternative function with subjective penalty for errors. In order to assess whether the performance of the participants differed in terms of the subjective cost they attributed to errors (accuracy bias) between the two conditions, we calculated the values of the parameter q corresponding to the error rates of each participant in both experimental and control sessions (see (4)) and compared them. The parameter q calculated for both the experimental (M = .47, SD = .40) and the control condition (M = .35, SD = .26) were significantly greater than 0, $t(23) = 4.13$, $p < .001$, and $t(23) = 4.26$, $p < .001$, respectively. This result indicates that regardless of the condition, participants had an accuracy bias. Consistent with our predictions, the weight assigned to accuracy relative to reward was significantly higher in the pre-SMA compared to the vertex inhibition condition, $t(23) = 2.35$, $p < .05$. Thus, under the right pre-SMA inhibition condition, participants displayed a significantly more cautious performance than the optimal (i.e., $q = 0$).

3.4. Post Error Slowing

In order to explore whether the increased cautiousness levels in the right pre-SMA inhibition condition was related to any change in the tendency of slowing down after erroneous responses (post error slowing - PES), we quantified PES as the difference in response times between the post-error trials and the post-correct trials. The difference between

post error and post correct response times (as a measure of PES) was significantly higher than 0 both in experimental ($t(23) = 3.05$, $p < .01$) and in control condition ($t(23) = 2.11$, $p < .05$). Although these results indicated that PES was evident within both conditions, there was not a significant difference between the two groups, $t(23) = .78$, $p = .44$. An estimated Bayes factor revealed that the odds were 3.53:1 in favor of the null hypothesis, providing substantial evidence for that there was no difference between groups.

The behavioral results gathered based on an alternative quantification method for PES (Dutilh et al., 2012) corroborated these results. As an alternative to the standard method, we quantified post-error slowing by calculating the difference between the post-error and the pre-error response times. This method was developed by Dutilh et al. (2012) who demonstrated that the standard method might cause spurious observation or masking of post-error slowing since it might be affected by global fluctuations in performance. Similar results were obtained from these set of analyses indicating that the difference between the post-error response times and the pre-error response times were significantly higher than the value of 0 both in the pre-SMA ($M = 0.11$, $SD = 0.21$), $t(23) = 2.54$, $p = .02$, and the vertex inhibition sessions ($M = 0.06$, $SD = 0.10$), $t(23) = 3.16$, $p = .004$. There was no significant difference between conditions, $t(23) = 1.30$, $p = .21$. We also conducted a Bayesian t-test which showed that the odds were 2.21:1 in favor of the null hypothesis (weak evidence) indicating that there was no difference between pre-SMA and vertex inhibition conditions in terms of PES scores.

In order to examine whether there were any difference in threshold setting between post-correct and post-error trials, and whether this difference varied between pre-SMA and vertex stimulation conditions, we fit a drift-diffusion model to the data allowing only the decision threshold parameter to vary. The results of this analysis revealed a higher threshold setting for post-error trials compared to post-correct trials regardless of the stimulation condition (see Figure 7A). However, the stimulation site did not have a differential effect on

the difference between post-error and post-correct trials in terms of post-error threshold setting (64% of posterior > 0; see Figure 7B).

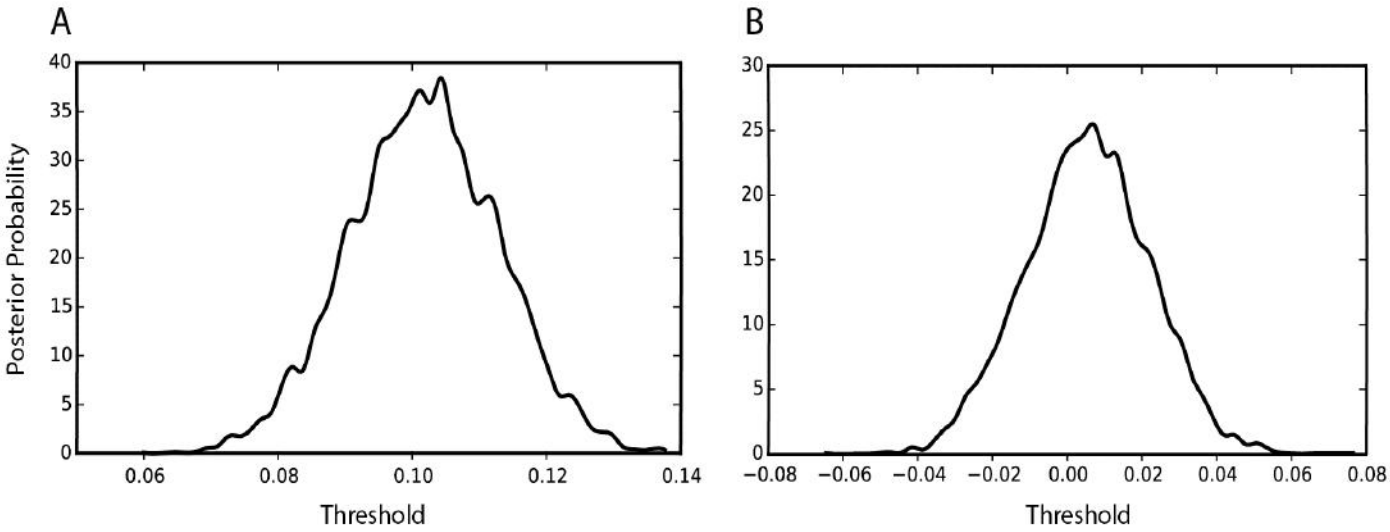

Figure 7. Posterior distribution of the threshold parameter estimated for post-error trials with regard to the post-correct trials (A) and the differential effect of the rTMS conditions on the difference between post-error and post-correct trials (B). Peak values of the distributions represent the best estimates of the parameter, and the width of the distributions represents its uncertainty.

We also investigated whether the accuracy of decisions increased after errors by comparing post-correct and post-error accuracy rates. The results indicated no significant difference between post-correct post-error accuracy rates, $F(1,23) = 3.05$, $p = .09$. Also, the stimulation condition (i.e., pre-SMA vs. vertex) did not have a differential effect on the difference in the accuracy rates between post-error and post-correct trials, $F(1,23) = 0.13$, $p = .72$.

DISCUSSION

In the current study, we investigated whether there is a causal relationship between the activity of right pre-SMA and control of the speed-accuracy tradeoff (SAT) in human

perceptual decision making without differentially emphasizing speed vs. accuracy. To this end, we examined the effect of the changes in the activity of right pre-SMA on decision thresholds estimated by the drift diffusion model. Based on earlier neuroimaging studies, we predicted that the inhibition of right pre-SMA would result in higher threshold setting and accuracy bias. The results of this study revealed that humans exhibit more cautious choice behavior by setting higher decision thresholds as a result of right pre-SMA inhibition compared to the inhibition of a control region (i.e., vertex). This difference was present despite the lack of significant differences as a result of isolated analysis of the accuracy and response times. This fact particularly reflects the importance of model-based approaches in cognitive neuroscience research (Erhan & Balcı, 2015; Forstmann & Wagenmakers, 2015).

As a mechanistic explanation for the change in cautiousness levels of the participants, we proposed that the inhibition of right pre-SMA exerts its downstream effect on the related cortico-basal ganglia pathways. Based on the striatal theory of the control of SAT, an increase in the activity of cortical non-integrator neurons (as in pre-SMA) excites striatum, which in turn decreases the inhibitory effect of the output nuclei of basal ganglia (globus pallidus) over the cortical areas related to motor execution (Bogacz et al., 2010a; Forstmann et al., 2008). This would enable globus pallidus to maintain/increase its inhibitory control over cortical areas based on the striatal theory of SAT (Forstmann et al., 2010). Thus, as a result of increased right pre-SMA activity, humans execute faster but often premature responses. With the same line of reasoning, the inhibition of right pre-SMA decreases the inhibitory effect of the striatum on basal ganglia. This in turn leads to a decreased activity in thalamus, resulting in a more cautious decision strategy (i.e., increased threshold setting).

Along with the increase in the decision thresholds, we also found that the weight assigned to accuracy relative to reward (i.e., accuracy bias) was significantly higher in the right pre-SMA compared to the vertex inhibition condition. This result reflects the effect of

right pre-SMA inhibition at the level of behavioral output when it is evaluated with respect to optimality benchmark.

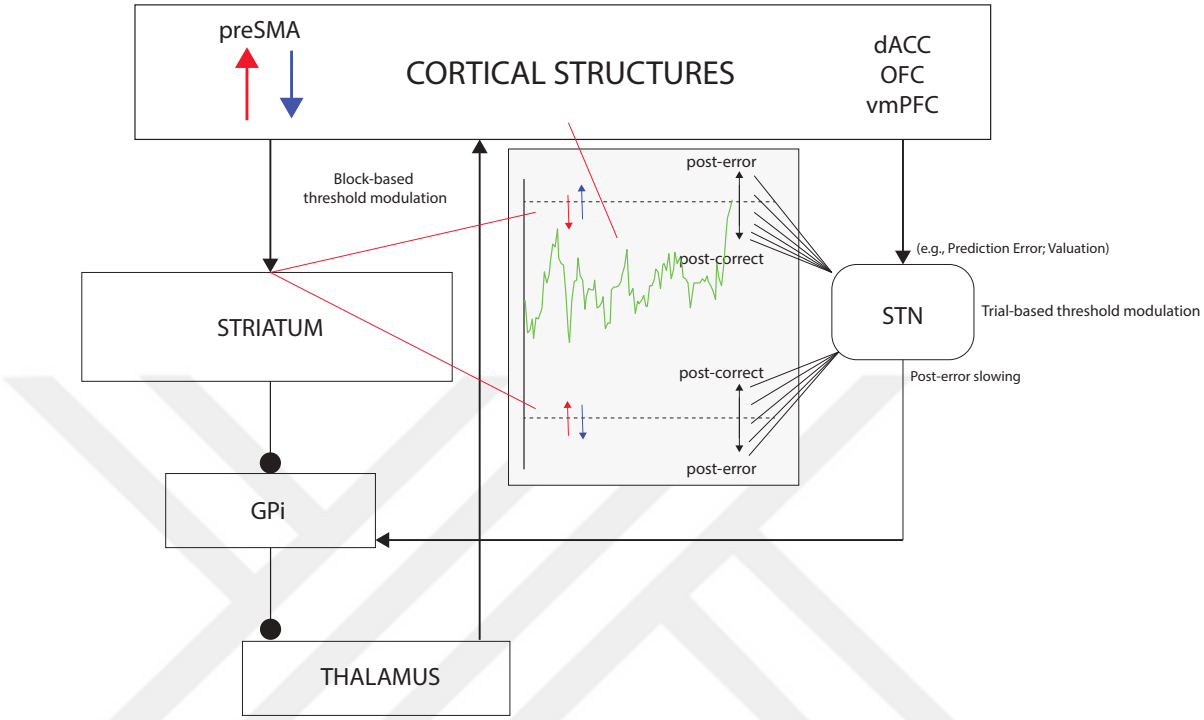

Figure 8. A possible neural mechanism for the block-based (macro-adaptive) and trial-based (micro-adaptive) modulation of decision thresholds. Pre-SMA-striatal pathway is implicated for macro-adaptive (based on global reward rate) whereas OFC/vmPFC-STN pathway is implicated for micro-adaptive (based on instantaneous outcome) modulation of decision-thresholds.

Another point of interest was the possible relationship between post-error slowing (PES) and SAT, since the underlying neural mechanisms of PES also include similar cortical and subcortical structures of the right hemisphere (Danielmeier & Ullsperger, 2011). In the review by Danielmeier and Ullsperger (2011), a network consisting of pre-SMA, lateral inferior frontal areas and the subthalamic nucleus (STN) are suggested to be crucial for PES. In the hyperdirect pathway, STN receives direct input from the cortex and projects directly to

the GPi to act as a global brake on the striatal output (Cavanagh et al., 2014). Thus, increased STN activity following erroneous responses enables acting more cautious in the next trial. In our study, a set of analyses related to PES indicated that within both conditions, participants responded slower by setting higher thresholds after they made an error, however this slowing or thresholds did not differ between the conditions. Thus, participants did not exhibit differential post-error behavior in terms of the speed of their decisions in the right pre-SMA inhibition condition compared to the control condition. Consequently, these findings indicated that while the baseline decision thresholds (presumably set based on global reward rate estimates), which control SAT, were affected by the right pre-SMA inhibition, no such differential modulation was observed in PES or associated transient changes in decision thresholds as a result of the change in activity in this area. In light of the findings of a previous study that indicated no effect of pre-SMA rTMS on the activity of STN (Watanabe et al., 2015), we can speculate that in our study pre-SMA inhibition did not modulate the activity of STN and therefore did not specifically lead to the modulation of PES. Overall our findings could be better accounted for by the striatal theory of SAT over STN theory.

The specificity of the effects of pre-SMA rTMS on average threshold values but not on post-error slowing (which has been previously attributed to wider threshold setting following errors) coupled with previous neuroimaging studies provide insights regarding the neural mechanisms that might differentially underlie macro-adaptive (block-based) vs. micro-adaptive (trial-based) modulation of decision thresholds. We propose that block-based threshold setting (for which SNR and average reward structure are relevant) and trial-based threshold modulation (for which the instantaneous consequences/outcomes of previous decisions are relevant) rely on partially dissociable networks. Specifically, we propose that pre-SMA-striatal pathway is associated with macro-adaptive threshold modulation whereas OFC/dACC/vmPFC-STN pathway is associated with micro-adaptive threshold modulation.

The latter process might be driven/guided by prediction error signals (Gehring & Willoughby 2002; Matsumodo & Takada, 2013; Roy et al., 2014; Seidler et al., 2013). To this end, particularly the OFC and vmPFC are likely candidate cortical structures that modulate STN's activity based on negative prediction errors (lower than average reward rate in erroneous decisions) that would lead to PES. The innervation of STN by substantia nigra pars compacta and VTA might on the other hand bring performance back to baseline following accurate decisions. Briefly, according to this account preSMA-striatal pathway would determine the baseline level of threshold setting (and set a lower limit) whereas cortical-STN pathway would modulate these thresholds from one trial to the next depending on the consequence of the previous decision. The integration of these two separate sources of signals takes place at the common efferent locus of these pathways, the globus pallidus interna. Figure 8 illustrates this model. Future studies may investigate these relationships using functional imaging methods.

A weakness of the current study could be related to the technique used for the localization of the target brain regions. We determined the stimulation sites (Fz for pre-SMA, Cz for vertex) based on the previous studies, which used the international 10-20 EEG system for pre-SMA localization (Hsu et al., 2011; Cavazzana et al., 2015). Before using the anatomical sites, we further considered whether the Talaraich coordinates of right pre-SMA determined by the previous studies (Chen et al., 2009; Conte et al., 2012; Li et al., 2006) fall within the stimulation sites (Fz and Cz) both in 10-10 system (Koessler et al., 2009) and in 10-20 system (Vitali et al., 2002). Moreover, we kept the number of participants much higher compared to the functional and structural MRI-guided TMS studies to increase the efficacy of our localization method (Sack et al., 2009). In a future study, the current study could be replicated with a smaller sample using MRI-guided localization techniques. Additionally, as we used only inhibition in the current study, the effect of pre-SMA facilitation on decision

thresholds could be investigated to examine whether increased pre-SMA activity leads to lower decision thresholds and more impulsive decisions.

REFERENCES

Aron AR, Poldrack RA. 2006. Cortical and subcortical contributions to stop signal response inhibition: role of the subthalamic nucleus. *J Neurosci* 26(9):2424-33. doi:10.1523/JNEUROSCI.4682-05.2006.

Bogacz R, Brown E, Moehlis J, Holmes P, Cohen JD. 2006. The physics of optimal decision making: A formal analysis of models of performance in two-alternative forced-choice tasks. *Psychol Rev* 113(4):700-65. doi:10.1037/0033-295X.113.4.700.

Bogacz R, Gurney K. 2007. The basal ganglia and cortex implement optimal decision making between alternative actions. *Neural Comput* 19(2):442-77. doi:10.1162/neco.2007.19.2.442.

Bogacz R, Wagenmakers EJ, Forstmann BU, Nieuwenhuis S. 2010a. The neural basis of the speed–accuracy tradeoff. *Trends Neurosci* 33(1):10-16. doi:10.1016/j.tins.2009.09.002.

Bogacz R, Hu PT, Holmes PJ, Cohen JD. 2010b. Do humans produce the speed–accuracy trade-off that maximizes reward rate? *Q J Exp Psychol (Hove)* 63(5):863-91. doi:10.1080/17470210903091643.

Brainard DH. 1997.The psychophysics toolbox. *Spat Vis* 10:433-6. doi:10.1163/156856897X00357.

Breysse E, Pelloux Y, Baunez C. 2015. The good and bad differentially encoded within the subthalamic nucleus in rats. *eNeuro* 2(5):1-17. doi:10.1523/ENEURO.0014-15.2015.

Brown JW, Bullock D, Grossberg S. 2004. How laminar frontal cortex and basal ganglia circuits interact to control planned and reactive saccades. *Neural Netw* 17(4):471-510. doi:10.1016/j.neunet.2003.08.006

Brown SD, Heathcote A. 2008. The simplest complete model of choice response time: Linear ballistic accumulation. *Cogn Psychol* 57(3):153-78. doi:10.1016/j.cogpsych.2007.12.002.

Burnham KP, Anderson DR. 2003. *Model selection and multimodel inference: a practical information-theoretic approach*. New York: Springer.

Cavanagh JF, Sanguinetti JL, Allen JJ, Sherman SJ, Frank MJ. 2014. The subthalamic nucleus contributes to post-error slowing. *J Cogn Neurosci* 26(11):2637-44. doi:10.1162/jocn_a_00659.

Cavazzana A, Penolazzi B, Begliomini C, Bisiacchi PS. 2015. Neural underpinnings of the 'agent brain': New evidence from transcranial direct current stimulation. *Eur J Neurosci* 42(3):1889-94. doi:10.1111/ejn.12937.

Chen CY, Muggleton NG, Tzeng OJ, Hung DL, Juan CH. 2009. Control of prepotent responses by the superior medial frontal cortex. *Neuroimage* 44(2):537-45. doi:10.1016/j.neuroimage.2008.09.005.

Chevalier G, Vacher S, Deniau JM, Desban M. 1985. Disinhibition as a basic process in the expression of striatal functions. I. The striato-nigral influence on tecto-spinal/tecto-diencephalic neurons. *Brain Res* 334(2), 215-26. doi:10.1016/0006-8993(85)90213-6.

Conte A, Rocchi L, Nardella A, Dispenza S, Scontrini A, Khan N, Berardelli A. 2012. Theta-burst stimulation-induced plasticity over primary somatosensory cortex changes

somatosensory temporal discrimination in healthy humans. *PLoS One* 7(3):32979. doi:10.1371/journal.pone.0032979.

Danielmeier C, Ullsperger M. 2011. Post-error adjustments. *Front Psychol* 2:233. doi:10.3389/fpsyg.2011.00233.

Deniau JM, Chevalier G. 1985. Disinhibition as a basic process in the expression of striatal functions. II. The striato-nigral influence on thalamocortical cells of the ventromedial thalamic nucleus. *Brain Res* 334(2):227-33. doi:10.1016/0006-8993(85)90214-8.

DeLong MR, Wichmann T. 2007. Circuits and circuit disorders of the basal ganglia. *Arch Neurol* 64(1):20-24. doi:10.1001/archneur.64.1.20.

Ding L, Gold JI. 2010. Caudate encodes multiple computations for perceptual decisions. *The J Neurosci* 30(47):15747-59. doi:10.1523/JNEUROSCI.2894-10.2010

Duecker F, Sack AT. 2013. Pre-stimulus sham TMS facilitates target detection. *PloS One* 8(3), e57765. doi:10.1371/journal.pone.0057765.

Dutilh G, Vandekerckhove J, Forstmann BU, Keuleers E, Brysbaert M, Wagenmakers EJ. 2012. Testing theories of post-error slowing. *Atten Percept Psychophys* 74(2):454-65. doi:10.3758/s13414-011-0243-2.

Erhan, C., & Balcı, F. 2015. Obsessive compulsive features predict cautious decision strategies. *Q J Exp Psychol*, 1-29. DOI: 10.1080/17470218.2015.1130070.

Fitts PM. 1966. Cognitive aspects of information processing: III. Set for speed versus accuracy. *J Exp Psychol* 71(6):849-57.

Forstmann BU, Wagenmakers EJ. 2015. Model-based cognitive neuroscience: A conceptual introduction. In: Forstman BU, Wagenmakers EJ, editors. *An introduction to model-based cognitive neuroscience*. New York:Springer. p139-56.

Forstmann BU, Anwander A, Schäfer A, Neumann J, Brown S, Wagenmakers EJ, Bogacz R, Turner R. 2010. Cortico-striatal connections predict control over speed and accuracy in perceptual decision making. *Proc Natl Acad Sci USA* 107(36):15916-20. doi:10.1073/pnas.1004932107.

Forstmann BU, Dutilh G, Brown S, Neumann J, Von Cramon DY, Ridderinkhof KR, Wagenmakers EJ. 2008. Striatum and pre-SMA facilitate decision-making under time pressure. *Proc Natl Acad Sci USA* 105(45):17538-42. doi:10.1073/pnas.0805903105

Frank MJ. 2006. Hold your horses: a dynamic computational role for the subthalamic nucleus in decision making. *Neural Netw* 19(8):1120-36. doi:10.1016/j.neunet.2006.03.006.

Frank MJ, Gagne C, Nyhus E, Masters S, Wiecki TV, Cavanagh JF, Badre D. 2015. fMRI and EEG predictors of dynamic decision parameters during human reinforcement learning. *J Neurosci* 35(2):485-94. doi: 10.1523/JNEUROSCI.2036-14.2015.

Frank MJ, Scheres A, Sherman SJ. 2007. Understanding decision-making deficits in neurological conditions: Insights from models of natural action selection. *Phil Trans R Soc B* 362(1485):1641-54. doi:10.1098/rstb.2007.2058.

Gehring WJ, Willoughby AR. 2002. The medial frontal cortex and the rapid processing of monetary gains and losses. *Science* 295(5563):2279:82. doi:10.1126/science.1066893.

Green N, Biele GP, Heekeren HR. 2012. Changes in neural connectivity underlie decision threshold modulation for reward maximization. *J Neurosci* 32(43):14942-50. doi:10.1523/JNEUROSCI.0573-12.2012.

Gurney K, Prescott TJ, Wickens JR, Redgrave P. 2004. Computational models of the basal ganglia: from robots to membranes.*Trends Neurosci* 27(8):453-9. doi:10.1016/j.tins.2004.06.003.

Herwig U, Satrapi P, Schönfeldt-Lecuona C. 2003.Using the international 10-20 EEG system for positioning of transcranial magnetic stimulation. *Brain Topogr* 16(2):95-99. doi:10.1023/B:BRAT.0000006333.93597.9d.

Hikosaka O, Isoda M. 2010. Switching from automatic to controlled behavior: cortico-basal ganglia mechanisms. *Trends Cogn Sci* 14(4):154-61. doi:10.1016/j.tics.2010.01.006.

Horvath JC, Forte JD, Carter O. 2014 Evidence that transcranial direct current stimulation (tDCS) generates little-to-no reliable neurophysiologic effect beyond MEP amplitude modulation in healthy human subjects: A systematic review. *Neuropsychologia*:1–24.

Hsu TU, Tseng LY, Yu JX, Kuo WJ, Hung DL, Tzeng OJL, Walsh V, Mugletton NG, Jian CH. 2011. Modulating inhibitory control with direct current stimulation of the superior medial frontal cortex. *Neuroimage* 56(4):2249-57. doi:10.1016/j.neuroimage.2011.03.059.

Huang YZ, Edwards MJ, Rounis E, Bhatia KP, Rothwell JC. 2005. Theta burst stimulation of the human motor cortex. *Neuron* 45(2):201-6. doi:10.1016/j.neuron.2004.12.033.

Hubl D, Nyffeler T, Wurtz P, Chaves S, Pflugshaupt T, Lüthi M, von Wartburg R, Wiest R, Dierks T, Strik WK, Hess CW, Müri RM. 2008. Time course of blood oxygenation level–dependent signal response after theta burst transcranial magnetic stimulation of the frontal eye field. *Neuroscience* 151(3):921-8. doi:10.1016/j.neuroscience.2007.10.049.

Ivanoff J, Branning P, Marois R. 2008. fMRI evidence for a dual process account of the speed-accuracy tradeoff in decision-making. *PLoS One* 3(7):e2635. doi:10.1371/journal.pone.0002635.

Koessler L, Maillard L, Benhadid A, Vignal JP, Felblinger J, Vespignani, Braun M. 2009. Automated cortical projection of EEG sensors: anatomical correlation via the international 10–10 system. *Neuroimage* 46(1):64-72. doi:10.1016/j.neuroimage.2009.02.006.

Laming DRJ. 1968. Information theory of choice-reaction times. Oxford: Acamedic Press.

Li CSR, Huang C, Constable RT, Sinha R. 2006. Imaging response inhibition in a stop-signal task: neural correlates independent of signal monitoring and post-response processing. *J Neurosci* 26(1):186-92. doi:10.1523/JNEUROSCI.3741-05.2006.

Lo CC, Wang XJ. 2006. Cortico–basal ganglia circuit mechanism for a decision threshold in reaction time tasks. Nat Neurosci 9(7):956-63. doi:10.1038/nn1722.

Maddox WT, Bohil CJ. 1998.Overestimation of base-rate differences in complex perceptual categories. *Percept Psychophys* 60(4):575-92. doi:10.3758/BF03206047.

Mansfield EL, Karayanidis F, Jamadar S, Heathcote A, Forstmann BU. 2011. Adjustments of response threshold during task switching: a model-based functional magnetic resonance imaging study. *J Neurosci* 31(41):14688-92. doi:10.1523/JNEUROSCI.2390-11.2011.

Matsumoto M, Takada M. 2013. Distinct representations of cognitive and motivational signals in midbrain dopamine neurons. *Neuron* 79(5):1011-24. doi:10.1016/j.neuron.2013.07.002.

Nachev P, Kennard C, Husain M. 2008.Functional role of the supplementary and pre-supplementary motor areas. *Nat Rev Neurosci* 9(11):856-69. doi:10.1038/nrn2478

Pelli DG. 1997. The VideoToolbox software for visual psychophysics: Transforming numbers into movies. *Spat Vis* 10(4):437-442. doi:10.1163/156856897X00366.

Pitz GF, Reinhold H. 1968. Payoff effects in sequential decision-making. *J Exp Psychol* 77(2):249-57. doi:10.1037/h0025802.

Raftery, A. E. 1995. Bayesian model selection in social research.*Sociological methodology*, *25*, 111-164.

Ratcliff R. 1978. A theory of memory retrieval. *Psychol Rev* 85(2):59. doi:10.1037/0033-295X.85.2.59.

Ratcliff R, McKoon G. 2008. The diffusion decision model: theory and data for two-choice decision tasks. *Neural Comput* 20(4):873-922. doi:10.1162/neco.2008.12-06-420.

Redgrave P, Prescott TJ, Gurney K.1999. The basal ganglia: a vertebrate solution to the selection problem? *Neuroscience* 89(4):1009-23. doi:10.1016/S0306-4522(98)00319-4.

Roitman JD, Shadlen MN. 2002. Response of neurons in the lateral intraparietal area during a combined visual discrimination reaction time task. *J Neurosci* 22(21):9475-89. doi:10.3410/f.1002839.152957.

Rouder JN, Speckman PL, Sun D, Morey RD, Iverson G. 2009. Bayesian t tests for accepting and rejecting the null hypothesis. *Psychon Bull Rev* 16:225–37. doi:10.3758/PBR.16.2.225.

Rossi, S., Hallett, M., Rossini, P. M., Pascual-Leone, A., & Safety of TMS Consensus Group. 2009. Safety, ethical considerations, and application guidelines for the use of transcranial magnetic stimulation in clinical practice and research. *Clin Neurophysiol.120*(12), 2008-2039. doi:10.1016/j.clinph.2009.08.016

Roy M, Shohamy D, Daw N, Jepma M, Wimmer GE, Wager TD. 2014. Representation of aversive prediction errors in the human periaqueductal gray. *Nat Neurosci* 17(11):1607-12. doi:10.1038/nn.3832.

Sack AT, Kadosh RC, Schuhmann T, Moerel M, Walsh V, Goebel R. 2009.Optimizing functional accuracy of TMS in cognitive studies: A comparison of methods. *J Cogn Neurosci* 21(2):207-21. doi:10.1162/jocn.2009.21126.

Seidler RD, Kwak Y, Fling BW, Bernard JA. 2013. Neurocognitive mechanisms of error-based motor learning. *Adv Exp Med Biol* 782:39-60. doi:10.1007/978-1-4614-5465-6_3.

Shadlen MN, Newsome WT. 2001. Neural basis of a perceptual decision in the parietal cortex (area LIP) of the rhesus monkey. *J Neurophysiol* 86(4):1916-36.

Standage D, Blohm G, Dorris MC. 2014. On the neural implementation of the speed-accuracy trade-off. *Front Neurosci* 8(236):10-3389. doi:10.3389/fnins.2014.00236.

Stevenson MK, Busemeyer JR, Naylor JC. 1991. Judgment and decision-making theory. In: Dunnette M, Hough LM, editors. *New handbook of industrial-organizational psychology*. Palo Alto:Consulting Psychologists Press.

Stone M. 1960. Models for choice-reaction time. Psychometrika 25(3):251-60.

Tremblay S, Lepage J-F, Latulipe-Loiselle A, Fregni F, Pascual-Leone A, Théoret H. 2014. The uncertain outcome of prefrontal tDCS. *Brain Stimulation* 7:773–783.

van Veen V, Krug MK, Carter CS. 2008. The neural and computational basis of controlled speed-accuracy tradeoff during task performance. *J Cogn Neurosci* 20(11):1952-65. doi:10.1162/jocn.2008.20146.

Vitali P, Avanzini G, Caposio L, Fallica E, Grigoletti L, Maccagnano E, Rigoldi B, Villani F. 2002. Cortical location of 10–20 system electrodes on normalized cortical MRI surfaces. *Int J Bioelectromagnetism* 4(2):147-8.

Wald A, Wolfowitz J. 1948. Optimum character of the sequential probability ratio test. *The Annals of Mathematical Statistics* 326-339.

Wassermann EM. 1998. Risk and safety of repetitive transcranial magnetic stimulation: report and suggested guidelines from the International Workshop on the Safety of Repetitive Transcranial Magnetic Stimulation, June 5–7, 1996. *Electroencephalography and Clinical Neurophysiology/Evoked Potentials Section*, 108(1):1-16.

Watanabe T, Hanajima R, Shirota Y, Tsutsumi R, Shimizu T, Hayashi T, Terao Y, Ugawa Y, Katsura M, Kunimatsu A, Ohtomo K, Hirose S, Miyashita Y, Konishi S. 2015. Effects of rTMS over pre-supplementary motor area on fronto-basal-ganglia network activity during stop-signal task. *J Neurosci* 35:4813-23. doi:10.1523/JNEUROSCI.3761-14.2015.

Wenzlaff, H., Bauer, M., Maess, B., & Heekeren, H. R. 2011. Neural characterization of the speed–accuracy tradeoff in a perceptual decision-making task. *J Neurosci*, *31*(4), 1254-1266. DOI:10.1523/JNEUROSCI.4000-10.2011.

Wickelgren WA. 1977. Speed-accuracy tradeoff and information processing dynamics. *Actapsychologica* 41(1):67-85. doi:10.1016/0001-6918(77)90012-9

Wiecki TV, Sofer I, Frank MJ. 2013. HDDM: Hierarchical bayesian estimation of the drift-diffusion model in python. *Front Neuroinform* 7:14. doi:10.3389/fninf.2013.00014.